

Design of Wideband Filtering Power Dividers with Harmonic Suppression Based on the Parallel-Coupled Line Structures

Xi Yu, Sheng Sun, and Yun Liu

School of Electronic Science and Engineering
University of Electronic Science and Technology of China, Chengdu, 611731, China
sunsheng@ieee.org

Abstract — This paper presents a wideband filtering power divider with harmonic suppression. By embedding two coupled-line sections to each way of the conventional Wilkinson structure, four resonant modes excited by two coupled lines and one original mode of the Wilkinson structure are incorporated to improve the in-band filtering responses. In order to enhance the frequency selectivity, a pair of long open stubs are inserted between these coupled-line sections to produce a pair of transmission zeros on both sides of the passband. Meanwhile, two additional transmission zeros at the upper stopband can be introduced to broaden the bandwidth of the stopband. Moreover, a short open stub is installed at the input port, which can also introduce one transmission zero to enhance upper stopband rejection. Finally, a prototype of the wideband filtering power divider operating at the center frequency of 3 GHz is designed and fabricated. The measured results show a 15-dB bandwidth of 56%, an isolation better than 18-dB and a 35-dB wide stopband from 4.44 to 7.73 GHz.

Index Terms — Coupled line, filtering power divider, harmonic suppression, wideband.

I. INTRODUCTION

In the modern wireless communication system, power dividers and filters as indispensable components have been widely used in the RF front ends of both receivers and transmitters. In order to meet the demands of high integration and multiple function, the filtering power dividers which combine both characteristics of filters and power dividers have attracted much attention in recent years.

To realize the filtering function, the techniques of coupling matrix and J/K inverter for the filter design can be applied to the filtering power divider design [1, 2]. Based on the coupling coefficients, a compact power divider with Chebyshev filtering response was implemented by using folded net-type resonators [1]. Although a good in-band isolation can be achieved, the frequency selectivity is poor. In order to achieve a high selectivity, the K -inverters implemented by dual-path

coupling structure were proposed to produce two transmission zeros on both sides of the passband and provide arbitrary power ratios at the same time [2]. In addition, E-shaped dual-mode resonators [3] and quarter-mode substrate integrated waveguide (SIW) circular cavities [4] were utilized to further reduce the circuit size. Nevertheless, the existing harmonic at upper stopband could degrade the out-of-band performance of the system. Therefore, the mixed electric and magnetic couplings as well as the cross coupling could be used to generate transmission zeros near the passband and the second harmonic [5]. Additionally, the discriminating coupling structure [6], short-circuited half-wavelength resonators [7] and open stubs [8] were also applied to achieve a wide upper stopband of the filtering power divider.

For the wideband applications, the hybrid slotline to microstrip line transition was proposed to be integrated with the Wilkinson power divider [9]. Although the response is ultra-wideband [9, 10], the out of band rejection level is not enough. By utilizing the first few resonant modes, the multi-mode resonator [11, 12] and ring resonator [13, 14] can be embedded to the power divider for a wide bandwidth and a filtering response. Since the coupled line provides not only a suitable coupling but also a filtering performance, it was often used to form the main structures of a wideband filtering power divider [15-18]. They can be installed at each port as matching networks to achieve a wideband response [15]. In [16], a pair of coupled lines terminated with open stubs were applied to replace the quarter-wavelength transmission lines in the conventional Wilkinson power dividers. A 70% fractional bandwidth can be achieved, whereas the out-of-band rejection level needs to be improved. Although the bandwidth and stopband suppression are acceptable by using the multi-sections quasi-coupled lines and short/open stubs [17], the in-band return loss was unsatisfactory. By utilizing two-sections coupled lines with center-loaded open stubs and two shorted stubs, the stopband can be extended [18]. On the other hand, the filtering power divider can be also designed to meet other special demands such as dual-

band [19, 20], balanced-to-balanced/unbalanced [21, 22], and multi-output [23-25].

In this paper, a wideband filtering power divider with wide stopband rejection is proposed. Conventionally, quarter-wavelength transmission lines are used in the design of Wilkinson power divider. By installing a short open stub at the input port, the required length of transmission lines can be shortened and a transmission zero would be produced at the upper stopband. Two coupled-line sections are embedded to each way of the power divider, which can excite four resonate modes. Together with the original mode of the Wilkinson structure, totally five transmission poles can be produced to construct a wideband filtering response. By choosing different even-odd mode impedances of embedded coupled lines, these resonate modes can be controlled to adjust the bandwidth of the filtering power divider. In addition, a long open stub is inserted between these two coupled lines, which not only considered provides the couplings between two coupled lines as a K -inverter [24], but also produces two transmission zeros on both sides of the passband to enhance the roll-off skirt. Meanwhile, two additional transmission zeros could also be produced at the upper stopband to broaden the bandwidth of upper stopband. These transmission zeros with the one produced by the short open stub can well suppress the harmonic and thus improve the upper stopband rejection. The theoretical analysis and design procedures are presented in the following sections in detail. To verify our proposal, a prototype of the wideband filtering power divider operating at center frequency of 3 GHz is finally designed, fabricated and measured. The measured results have good agreement with the simulated ones.

II. ANALYSIS AND DESIGN

Figure 1 shows the configuration of the two-way wideband filtering power divider. It consists of a transmission line, two section coupled lines and a long open stub in each way. A short open stub is loaded at the input port and a resistor R is connected between the two output ports. Z_i and Z_{ei} , Z_{oi} ($i = 1, 2$) are the characteristic impedances of the microstrip lines and the even-odd mode impedances of the coupled lines, while θ and θ_s are the electrical length of the corresponding transmission lines, respectively. In this work, θ is chosen to be $\theta_0 = \pi/2$, which is quarter-wavelength at the center operating frequency f_0 . For simplicity, the phase velocities of the even and odd modes are assumed to be the same so that the coupled line structures have the same even/odd-mode electrical length. Due to the fully symmetric structure, the proposed filtering power divider can be decomposed into two half equivalent circuits under the even and odd excitations, as shown in Figs. 2 (a) and (b). When the even mode is excited, the $ABCD$ -matrix of the half circuit model can be derived as:

$$[A]_e = \begin{bmatrix} A_e & B_e \\ C_e & D_e \end{bmatrix}. \quad (1)$$

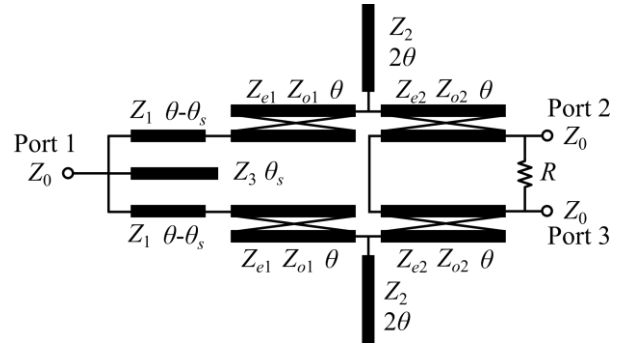


Fig. 1. The schematic of the proposed wideband filtering power divider.

Then, the S -parameters $[S^e]$ of the even-mode circuit with two different port impedances can be obtained by using the following relationships:

$$S_{11}^e = \frac{A_e Z_0 + B_e - 2C_e Z_0^2 - 2D_e Z_0}{A_e Z_0 + B_e + 2C_e Z_0^2 + 2D_e Z_0}, \quad (2)$$

$$S_{21}^e = \frac{2\sqrt{2}(A_e D_e - B_e C_e) Z_0}{A_e Z_0 + B_e + 2C_e Z_0^2 + 2D_e Z_0}, \quad (3)$$

$$S_{22}^e = \frac{-A_e Z_0 + B_e - 2C_e Z_0^2 + 2D_e Z_0}{A_e Z_0 + B_e + 2C_e Z_0^2 + 2D_e Z_0}. \quad (4)$$

On the other hand, when the odd mode is excited, the second coupled line is loaded with a short-circuited and an open-circuited terminations. The equivalent circuit of this coupled line is also shown in Fig. 2 (b). It can be found that the frequency response of this coupled line is all-stop. Therefore, the S -parameters $[S^o]$ of the single-port odd-mode circuit can be expressed as:

$$S_{22}^o = \frac{Z_{in} - Z_0}{Z_{in} + Z_0}, \quad (5)$$

where

$$Z_{in} = \frac{j2R(Z_{e2} + Z_{o2}) \tan \theta}{4R + j(Z_{e2} + Z_{o2}) \tan \theta}. \quad (6)$$

Based on the even-odd mode analysis, the S -parameters $[S]$ of the filtering power divider can be given as:

$$S_{11}(\theta) = S_{11}^e(\theta), \quad (7)$$

$$S_{12}(\theta) = S_{21}(\theta) = S_{13}(\theta) = S_{31}(\theta) = \frac{S_{21}^e(\theta)}{\sqrt{2}}, \quad (8)$$

$$S_{22}(\theta) = S_{33}(\theta) = \frac{S_{22}^e(\theta) + S_{22}^o(\theta)}{2}, \quad (9)$$

$$S_{23}(\theta) = S_{32}(\theta) = \frac{S_{22}^e(\theta) - S_{22}^o(\theta)}{2}, \quad (10)$$

and the S_{11} can be further written as:

$$S_{11} = -\frac{k_1 \cos \theta_s + k_2 \sin \theta_s \tan \theta_s + jk_3 \sin \theta_s}{k_1 \cos \theta_s + k_2 \sin \theta_s \tan \theta_s + jk_4 \sin \theta_s}, \quad (11)$$

where

$$k_1 = Z_3 \left[2Z_0^2 (Z_{e1} - Z_{o1})^2 - Z_1^2 (Z_{e2} - Z_{o2})^2 \right],$$

$$k_2 = Z_0^2 Z_1 (Z_{e1} - Z_{o1})^2,$$

$$k_3 = Z_0 Z_1 [(Z_1 - 2Z_3)(Z_{e2} - Z_{o2})^2 + Z_3 (Z_{e1} - Z_{o1})^2],$$

$$k_4 = Z_0 Z_1 [(Z_1 - 2Z_3)(Z_{e2} - Z_{o2})^2 - Z_3 (Z_{e1} - Z_{o1})^2].$$

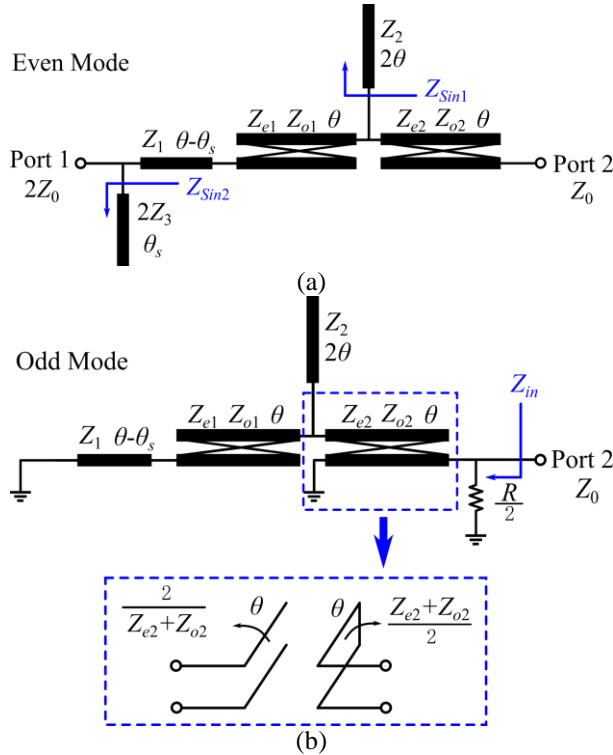


Fig. 2. The decomposed equivalent circuits of the filtering power divider. (a) Even-mode circuit model. (b) Odd-mode circuit model.

In order to achieve a good in-band return loss, we can solve the equation of $S_{11}(\theta) = 0$ at the center frequency. Then, Z_1 and Z_3 can be deduced as:

$$Z_1 = \frac{Z_0 \sqrt{2(Z_{e1} - Z_{o1})^2 + \left[2 - \left(\frac{Z_{e1} - Z_{o1}}{Z_{e2} - Z_{o2}} \right)^2 \right] \tan^2 \theta_s}}{Z_{e2} - Z_{o2}}, \quad (12)$$

$$Z_3 = \frac{Z_1 (Z_{e2} - Z_{o2})^2}{2(Z_{e2} - Z_{o2})^2 - (Z_{e1} - Z_{o1})^2}. \quad (13)$$

From (12) and (13), it can be noticed that once the even-odd mode impedances of the coupled lines are determined, Z_1 and Z_3 can be evaluated by choosing a

proper value of θ_s . According to (12) and (13), Z_1 and Z_3 increase as θ_s increases. When $\theta_s = 0$, Z_1 can be calculated as:

$$Z_1 = \sqrt{2} Z_0 \frac{Z_{e1} - Z_{o1}}{Z_{e2} - Z_{o2}}. \quad (14)$$

In this work, $(Z_{e1} - Z_{o1})$ is larger than $(Z_{e2} - Z_{o2})$. Therefore, compared with the conventional Wilkinson power divider, the value of Z_1 is larger than $\sqrt{2} Z_0$ due to the influence of the embedded coupled lines.

Figure 3 shows the S-parameters of the filtering power divider with different θ_s . The corresponding realizable characteristic impedances of each curve plotted in Fig. 3 are summarized in Table 1. As θ_s increases, the frequency response has little influence, as shown in Fig. 3. However, when θ_s increases to 60° , Z_3 becomes very large and exceeds the maximal realizable characteristic impedance of the microstrip line. Thus, the in-band response is deteriorated extremely. Considering that the maximal characteristic impedance of the realizable microstrip line on the substrate of RO4350B with a thickness of 0.508 mm and a dielectric constant of 3.66 is 134 Ohm, and $(Z_{e1} - Z_{o1})$ is about 100~107 Ohm, and $(Z_{e2} - Z_{o2})$ is 90~95 Ohm, the maximal θ_s is about 52° when the performance is acceptable and the impedance is realizable.

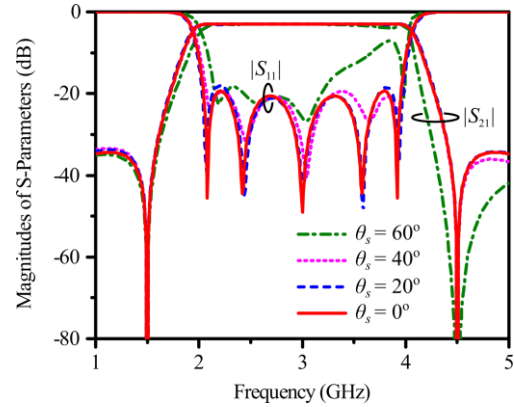


Fig. 3. The S-parameters of the wideband filtering power divider with different θ_s .

Table 1: The corresponding realizable characteristic impedances of the filtering power divider with different θ_s

θ_s	Z_1	Z_2	Z_3	Z_{e1}	Z_{o1}	Z_{e2}	Z_{o2}
0°	80	36	-	156	51	154	61
20°	82	36	120	157	51	155	61
40°	87	34	126	148	48	147	56
60°	105	26	134	134	45	136	53

As shown in Fig. 3, when θ_s equals to 0° , 20° , and 40° respectively, there are five transmission poles in the passband and two transmission zeros on two sides of the

passband. In comparison with the conventional Wilkinson power divider, the two embedded coupled lines can provide four in-band poles and the length of the conventional quarter-wavelength transmission line can be reduced to be $\pi/2 - \theta_s$. The two transmission zeros near the passband are introduced by loading the long open stubs between coupled lines. When the impedance of the long open stub equals to zero, the current of the circuit would be directly shorted to the ground, which can produce a transmission zero. Therefore, the location of these two transmission zeros can be found by solving the following equation:

$$Z_{sin1} = -jZ_2 \cot 2\theta = 0, \quad (15)$$

the positions are finally obtained as:

$$f_{s1n} = \frac{(2n-1) \cdot 90^\circ}{2\theta} f_0 = \frac{2n-1}{2} f_0 \quad (n=1, 2, \dots). \quad (16)$$

As it can be found in (15), the impedance of the open stub is a pure reactance or susceptance within the passband, which can be equivalent to a K -inverter [24]. Therefore, the two long open stubs can not only produce the out-of-band transmission zeros, but also can provide the in-band coupling between the two coupled lines as a K -inverter. Similar to the long open stub, the short open stub at the input port can also provide transmission zeros at higher frequency band. By solving the equation:

$$Z_{sin2} = -j2Z_3 \cot \theta_s = 0, \quad (17)$$

the locations of the transmission zeros can be obtained as:

$$f_{s2n} = \frac{(2n-1) \cdot 90^\circ}{\theta_s} f_0 \quad (n = 1, 2, \dots). \quad (18)$$

In order to improve the in-band isolation between two output ports, the resistor can be loaded and determined as $R = 2Z_0$ by letting $S_{23} = 0$.

Figure 4 illustrates the influence of Z_2 on the in-band response. As Z_2 increases, the reflection at port 2/3 is almost unchanged and in-band $|S_{22(33)}|$ is below -20 dB. However, the in-band performance of $|S_{11}|$ and $|S_{23}|$ are deteriorated near the edge frequency of the passband. Therefore, a proper value of Z_2 needs to be determined in order to achieve a good in-band return loss and isolation.

Figure 5 shows the influence of impedances on the bandwidth. Once the operating center frequency f_0 is chosen, the transmission zeros introduced by the long open stub are determined according to (16), and the passband of each way is limited between the first two transmission zeros. However, these transmission zeros cannot be independently controlled by only one open stub, so that the bandwidth cannot be adjusted by only changing the length of the long open stub. If the length is changed, these two transmission zeros can move at the same time and the operating center frequency of the passband f_0 is also shifted. Therefore, in order to maintain f_0 unchanged, the lengths of all the transmission lines are fixed and the impedances is utilized to control the

bandwidth of the filtering power divider. Three cases with $\theta_s = 0$ are given to demonstrate the bandwidth control with the different characteristic impedances of transmission lines, and the detail specifications and results are shown in Table 2. As illustrated in Fig. 5 and Table 2, Case III has a wider bandwidth than other two cases. Although the out-of-band rejection level and the in-band isolation is unsatisfactory compared with the others, a sharp roll-off skirt can be achieved. For the Case I, the bandwidth is narrower than Case II and III with very high even-odd mode impedances and low characteristic impedance of the long open stub (Z_3). It can be also found that as the increase of the bandwidth, Z_2 increases gradually while the other impedances decrease. Therefore, according to Table 2, different bandwidths can be achieved by choosing proper characteristic impedances with fixed electric length of the transmission lines.

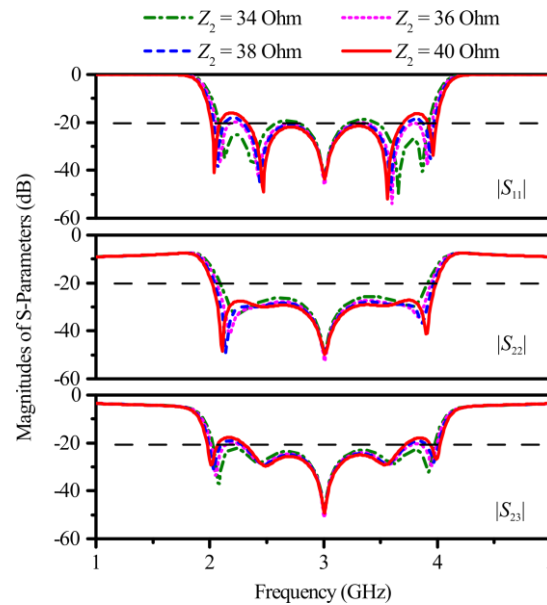


Fig. 4. The S-parameters of the wideband filtering power divider with different Z_2 when $\theta_s = 20^\circ$.

Finally, the design procedure of the proposed wideband filtering power divider can be summarized as follows:

- 1) Determine the operating center frequency f_0 and the positions of the two transmission zeros near the passband can be calculated by (16);
- 2) Choose the positions of the transmission zeros at the higher frequency band according to (18) and determine the θ_s ;
- 3) Based on Tables 1, 2, Fig. 4 and Fig. 5, choose the proper Z_2 and even-odd mode impedance of the coupled lines. According to (12) and (13), Z_1 and Z_3 can be determined;
- 4) Determine the isolation resistor $R=2Z_0$.

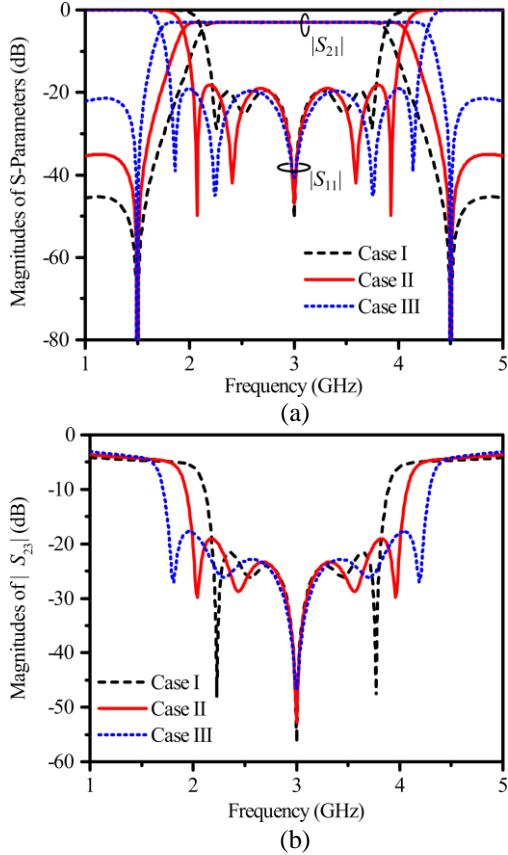


Fig. 5. The magnitudes of S-parameters for the Case I, II, and III. (a) The magnitudes of $|S_{11}|$ and $|S_{21}|$. (b) The magnitudes of $|S_{23}|$.

Table 2: The corresponding characteristic impedances and simulated results for Case I, II, and III

Case	Z_1	Z_2	Z_{e1}	Z_{o1}	Z_{e2}	Z_{o2}	FBW/ RL ¹	R ² / I ³
I	83	25	192	81	180	86	51.7%/ 19.6 dB	45 dB/ 21 dB
II	80	36	156	51	154	61	65.0%/ 18.0 dB	35 dB/ 19 dB
III	79	76	142	30	143	42	78.6%/ 19.5 dB	21 dB/ 17 dB

RL¹: return loss; R²: out-of-band rejection level; I³: in-band isolation

III. IMPLEMENT AND RESULTS

A prototype of the wideband filtering power divider is designed and fabricated on the substrate of RO4350B with a thickness of 0.508 mm and a dielectric constant of 3.66 at the operating center frequency of 3 GHz. In order to suppress the second harmonic around 6 GHz, θ_S is chosen as 45° , while the circuit size becomes smaller accordingly. The circuit layout and the photograph of the fabricated wideband filtering power divider are depicted in Fig. 6 and Fig. 7, respectively. In order to realize the high even-odd mode impedance and provide strong

couplings, two apertures are etched on the ground plane. vAs shown in Fig. 6, the main dimensions of the proposed wideband filtering power divider are finally optimized to be: $w_0 = 0.95$, $w_1 = 0.1$, $w_2 = 0.23$, $w_3 = 1.36$, $l_1 = 6.37$, $l_2 = 7.57$, $l_3 = 14.7$, $l_4 = 29.28$, $l_5 = 15.7$, $s_1 = 0.12$, and $s_2 = 0.11$ (units: mm). The isolation resistor is calculated as 100 Ohm. Figure 8 shows the circuit simulated frequency responses when θ_S is 0° and 45° respectively. It can be found that when there is no short open stub, the second harmonic is generated at 6 GHz. When θ_S is 45° , the harmonic at 6 GHz is suppressed by the transmission zero. However, the harmonic mode still exists and is pushed up to a higher frequency, so that there is a peak on S_{11} at 6.5 GHz. Although the harmonic mode still exists, the magnitude of S_{21} is pulled down below -20 dB due to the introduced transmission zero. Figure 9 shows the EM simulated surface current at 6.5 GHz. There is very strong current distribution on the short open stub and the first coupled-line section. Since the width of coupled lines is small and two apertures are just etched behind them on the ground plane to provide strong in-band couplings, some radiation from the apertures could happen at 6.5 GHz.

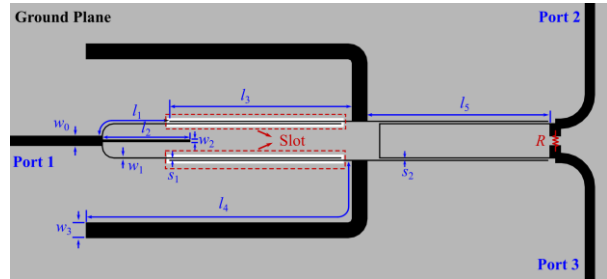


Fig. 6. The layout of the wideband filtering power divider.

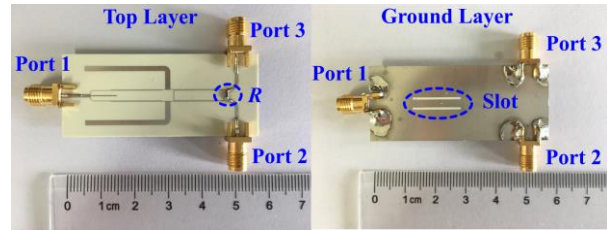


Fig. 7. The photograph of the fabricated wideband filtering power divider.

The full-wave simulated results and measured results are plotted in Fig. 10. The in-band return loss is better than 15 dB and the minimum insertion loss is -3-0.7 dB. The measured fractional bandwidth of 15-dB in-band return loss is about 56% over the frequency range from 2.30 to 3.98 GHz. The in-band isolation is better than

18 dB. In addition, a 35-dB harmonic suppression can be achieved at the stopband from 4.44 to 7.73 GHz, although the leakage from the apertures seems more obvious at 6.5 GHz. As shown in Fig. 10 (a), it can be noticed that there are six transmission zeros over the concerned frequency band. The first two transmission zeros (f_{tz1}, f_{tz2}) and the last one (f_{tz6}) are located at 1.5 GHz, 4.5 GHz and 7.5 GHz, which is introduced by the long open stub. f_{tz3} introduced by the short open stub is allocated at 6.18 GHz to suppress the second harmonic of the center frequency. Because of the existing of coupled lines, two more transmission zeros f_{tz4} and f_{tz5} are introduced at 6.73 GHz and 7.05 GHz. Owing to the four transmission zeros ($f_{tz3}, f_{tz4}, f_{tz5},$ and f_{tz6}) at the upper stopband, the spurious harmonic frequencies can be well suppressed and a wide stopband can be obtained. The magnitude and phase imbalance between two output ports are less than ± 0.2 dB and $\pm 1.3^\circ$, respectively, as depicted in Fig. 11 (a). Figure 11 (b) shows the in-band group delay of the filtering power divider. Comparison with the other design in previous work is tabulated in Table 3. It can be found that the proposed filtering power divider has achieved a wide bandwidth of 56%, a well harmonic suppression of 35 dB and six transmission zeros in total.

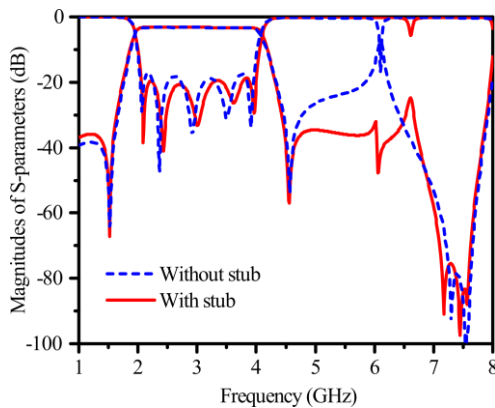


Fig. 8. The circuit simulated frequency responses of the filtering power divider with and without short open stub.

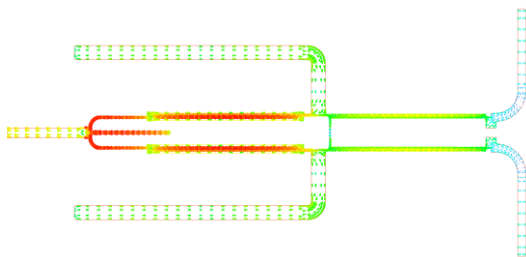


Fig. 9. The surface current of the filtering power divider at 6.5 GHz.

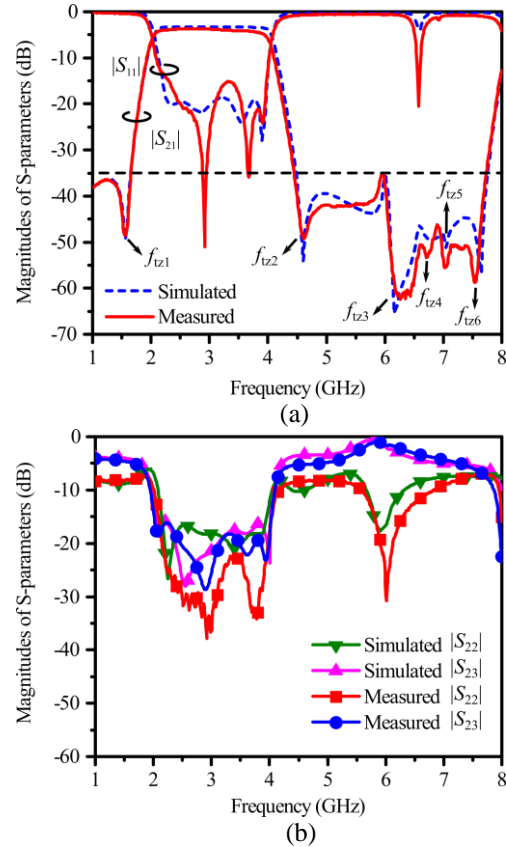


Fig. 10. The EM simulated and measured results of the wideband filtering power divider. (a) The magnitudes of S_{11} and S_{21} . (b) The magnitudes of S_{22} and S_{23} .

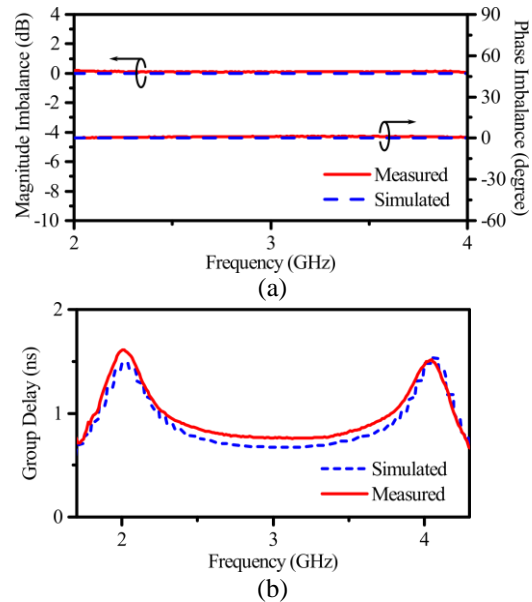


Fig. 11. (a) The in-band magnitude and phase imbalance. (b) The group delay of the filtering power divider.

Table 3: Comparison with the wideband filtering power divider in the literature

Ref.	f_0 (GHz)	FBW/RL ¹ (In-band)	BW/IL ² (Stopband)	Isolation	TZs ³
[8]	6.80	85.3% 15 dB	-	15.0dB	-
[9]	2.15	31.0% 17 dB	$4.2 f_0$ 20 dB	17.0 dB	2
[10]	2.05	62.0% 10.14 dB	$0.95 f_0$ 15.8 dB	10.0 dB	5
[11]	1.50	60% 14 dB	-	20 dB	2
[12]	2.00	62.0% 15 dB	-	20.0 dB	-
[13]	3.00	70.0% 20 dB	$2.6 f_0$ 13 dB	16.7 dB	4
[14]	3.00	104.5% 15 dB	$3.4 f_0$ 15 dB	15.0 dB	3
[15]	1.00	43.0 % 20 dB	$3.9 f_0$ 20 dB	20.0 dB	5
This work	3.00	56.0 % 15 dB	$1.1 f_0$ 35 dB	18.0 dB	6

¹RL: Return Loss; ²IL: Insertion Loss; ³TZs: Transmission zeros

IV. CONCLUSION

In this paper, a wideband filtering power divider with wide stopband has been proposed. Based on the two embedded coupled lines and long open stubs, the wideband filtering response has been achieved with a sharp roll-of skirt. The introduced short open stub at the input port not only reduced the length of the conventional quarter-wavelength in Wilkinson structure, but also provided a transmission zero at upper stopband to improve the out-of-band rejection level. With the help of total five resonances and six transmission zeros, a 56% bandwidth, a high 35-dB stopband rejection and an isolation better than 18 dB have been achieved.

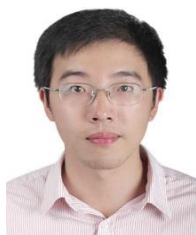
ACKNOWLEDGMENT

This work was supported by the National Natural Science Foundation of China No. 61622106 and No. 61721001.

REFERENCES

- [1] C. F. Chen and C. Y. Lin, "Compact microstrip filtering power dividers with good in-band isolation performance," *IEEE Microw. Wireless Compon. Lett.*, vol. 24, no. 1, pp. 17-19, Jan. 2014.
- [2] K. X. Wang, X. Y. Zhang, and B. J. Hu, "Gysel power divider with arbitrary power ratios and filtering responses using coupling structure," *IEEE Trans. Microw. Theory Techn.*, vol. 62, no. 3, pp. 431-440, Mar. 2014.
- [3] G. Zhang, J. Wang, L. Zhu, and W. Wu, "Dual-mode filtering power divider with high passband selectivity and wide upper stopband," *IEEE Microw. Wireless Compon. Lett.*, vol. 27, no. 7, pp. 642-644, July 2017.
- [4] X. Wang and X. W. Zhu, "Quarter-mode circular cavity substrate integrated waveguide filtering power divider with via-holes perturbation," *Electron. Lett.*, vol. 53, no. 12, pp. 791-793, June 8, 2017.
- [5] X. Y. Zhang, K. X. Wang, and B. J. Hu, "Compact filtering power divider with enhanced second-harmonic suppression," *IEEE Microw. Wireless Compon. Lett.*, vol. 23, no. 9, pp. 483-485, Sept. 2013.
- [6] X. L. Zhao, L. Gao, X. Y. Zhang, and J. X. Xu, "Novel filtering power divider with wide stopband using discriminating coupling," *IEEE Microw. Wireless Compon. Lett.*, vol. 26, no. 8, pp. 580-582, Aug. 2016.
- [7] W. M. Chau, K. W. Hsu, and W. H. Tu, "Wide-stopband Wilkinson power divider with bandpass response," *Electron. Lett.*, vol. 50, no. 1, pp. 39-40, Jan. 2, 2014.
- [8] M. Hayati and S. Roshani, "A novel Wilkinson power divider using open stubs for the suppression of harmonics," *ACES J.*, vol. 28, no. 6, pp. 501-506, June 2013.
- [9] K. Song, Y. Zhu, Q. Duan, M. Fan, and Y. Fan, "Extremely compact ultra-wideband power divider using hybrid slotline/microstrip-line transition," *Electron. Lett.*, vol. 51, no. 24, pp. 2014-2015, Nov. 19, 2015.
- [10] A. Piroutiniya and P. Mohammadi, "The substrate integrated waveguide T-junction power divider with arbitrary power dividing ratio," *ACES J.*, vol. 31, no. 4, pp. 428-433, Apr. 2016.
- [11] Y. Deng, J. Wang, and J.-l. Li, "Design of compact wideband filtering power divider with extended isolation and rejection bandwidth," *Electron. Lett.*, vol. 52, no. 16, pp. 1387-1389, Aug. 4, 2016.
- [12] Y. Deng, Y. He, and J. Wang, "Design of a compact wideband filtering power divider with improved isolation," *ACES J.*, vol. 31, no. 9, pp. 1079-1083, Sept. 2016.
- [13] S. S. Gao, S. Sun, and S. Xiao, "A novel wideband bandpass power divider with harmonic-suppressed ring resonator," *IEEE Microw. Wireless Compon. Lett.*, vol. 23, no. 3, pp. 119-121, Mar. 2013.
- [14] Y. Liu, S. Sun, and X. Yu, "Design of a wideband filtering power divider with stub-loaded ring resonator," in *Int. Applied Computational Electromagnetics Society Symp. (ACES-2017)*, Suzhou, China, Aug. 2017.
- [15] M. A. Maktoomi, M. S. Hashmi, and F. M. Ghannouchi, "Theory and design of a novel wide-band DC isolated Wilkinson power divider," *IEEE Microw. Wireless Compon. Lett.*, vol. 26, no. 8, pp. 586-588, Aug. 2016.
- [16] B. Zhang and Y. Liu, "Wideband filtering power

- divider with high selectivity," *Electron. Lett.*, vol. 51, no. 23, pp. 1950-1952, Nov. 5, 2015.
- [17] C. W. Tang and J. T. Chen, "A design of 3-dB wideband microstrip power divider with an ultra-wide isolated frequency band," *IEEE Trans. Microw. Theory Techn.*, vol. 64, no. 6, pp. 1806-1811, June 2016.
- [18] Y. Wu, Z. Zhuang, Y. Liu, L. Deng, and Z. Ghassemlooy, "Wideband filtering power divider with ultra-wideband harmonic suppression and isolation," *IEEE Access*, vol. 4, pp. 6876-6882, 2016.
- [19] G. Zhang, J. Wang, L. Zhu, and W. Wu, "Dual-band filtering power divider with high selectivity and good isolation," *IEEE Microw. Wireless Compon. Lett.*, vol. 26, no. 10, pp. 774-776, Oct. 2016.
- [20] C. Shao, Y. Li, and J. X. Chen, "Compact dual-band microstrip filtering power divider using T-junction structure and quarter-wavelength SIR," *Electron. Lett.*, vol. 53, no. 6, pp. 434-436, Mar. 16, 2017.
- [21] K. Xu, J. Shi, L. Lin, and J. X. Chen, "A balanced-to-unbalanced microstrip power divider with filtering function," *IEEE Trans. Microw. Theory Techn.*, vol. 63, no. 8, pp. 2561-2569, Aug. 2015.
- [22] X. Gao, W. Feng, W. Che, and Q. Xue, "Wideband balanced-to-unbalanced filtering power dividers based on coupled lines," *IEEE Trans. Microw. Theory Techn.*, vol. 65, no. 1, pp. 86-95, Jan. 2017.
- [23] P. H. Deng and Y. T. Chen, "New Wilkinson power dividers and their integration applications to four-way and filtering dividers," *IEEE Trans. Compon., Packag. Manuf. Technol.*, vol. 4, no. 11, pp. 1828-1837, Nov. 2014.
- [24] F. J. Chen, L. S. Wu, L. F. Qiu, and J. F. Mao, "A four-way microstrip filtering power divider with frequency-dependent couplings," *IEEE Trans. Microw. Theory Techn.*, vol. 63, no. 10, pp. 3494-3504, Oct. 2015.
- [25] H. Zhu, A. M. Abbosh, and L. Guo, "Wideband four-way filtering power divider with sharp selectivity and wide stopband using looped coupled-line structures," *IEEE Microw. Wireless Compon. Lett.*, vol. 26, no. 6, pp. 413-415, June 2016.



Xi Yu received the B.Eng. degree in Electronic Engineering from The University of Electronic Science and Technology of China (UESTC), Chengdu, China in 2013, and he is currently working towards the Ph.D. degree in UESTC. His research interests include the synthesis and

design of microwave filters and antennas, multifunctional integrated devices, as well as the wireless power transfer system.



Sheng Sun received the B.Eng. degree in Information Engineering from the Xi'an Jiaotong University, China, in 2001, and the Ph.D. degree in Electrical and Electronic Engineering from the Nanyang Technological University (NTU), Singapore, in 2006.

Sun was with the Institute of Microelectronics in Singapore (2005-2006), and with the NTU (2006-2008) as a Postdoc Research Fellow. He was also a Humboldt Research Fellow with the Institute of Microwave Techniques at the University of Ulm in Germany (2008-2010), and a Research Assistant Professor at The University of Hong Kong (2010-2015). Since 2015, he has been the Young Thousand Talents Plan Professor at The University of Electronic Science and Technology of China (UESTC). His research interests include electromagnetic theory and computational mathematics, multi-physics, numerical modeling of planar circuits and antennas, microwave passive and active devices, as well as the microwave and millimeter-wave communication systems. He has coauthored one book and two book chapters, over 140 journal and conference publications. He was a co-recipient of the several Best Paper Awards at international conferences. He received the Outstanding Reviewer Award from IEEE Microwave and Wireless Components Letters in 2010. He was the recipient of the General Assembly Young Scientists Award from the International Union of Radio Science (URSI) in 2014. He also received the Hildegard Maier Research Fellowship of the Alexander Von Humboldt Foundation (Germany), in 2008, and the recipient of the ISAP Young Scientist Travel Grant (Japan), in 2004. Sun was an Associate Editor of the IEICE Transactions on Electronics (2010-2014), a Guest Associate Editor of the ACES Journal (2017). He is currently a Member of Editor Board of International Journal of RFMiCAE and Journal of Communications and Information Networks, as well as an Associate Editor of IEEE Microwave and Wireless Components Letters.



Yun Liu received the B.Eng. degree in Electronic Engineering from The University of Electronic Science and Technology of China (UESTC), Chengdu, China in 2015, and she is currently pursuing the Ph.D. degree in UESTC. Her research interests include microwave power dividers, planar multifunctional microwave passive components, as well as patch antennas.